Electron collisions with the HCOOH···(H2O) n complexes (n = 1, 2) in liquid phase: The influence of microsolvation on the π* resonance of formic acid

T. C. Freitas, K. Coutinho, M. T. do N. Varella, M. A. P. Lima, S. Canuto, and M. H. F. Bettega

Citation: The Journal of Chemical Physics **138**, 174307 (2013); doi: 10.1063/1.4803119

View online: http://dx.doi.org/10.1063/1.4803119

View Table of Contents: http://scitation.aip.org/content/aip/journal/jcp/138/17?ver=pdfcov

Published by the AIP Publishing

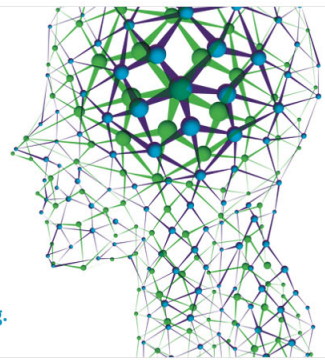

Electron collisions with the HCOOH···$(H_2O)_n$ complexes ($n = 1, 2$) in liquid phase: The influence of microsolvation on the π^* resonance of formic acid

T. C. Freitas,[1,2] K. Coutinho,[3] M. T. do N. Varella,[3] M. A. P. Lima,[4] S. Canuto,[3] and M. H. F. Bettega[2,a)]

[1]*Tecnologia em Luteria, Universidade Federal do Paraná, Rua Dr. Alcides Vieira Arcoverde 1255, 81520-260 Curitiba, Paraná, Brazil*
[2]*Departamento de Física, Universidade Federal do Paraná, Caixa Postal 19044, 81531-990 Curitiba, Paraná, Brazil*
[3]*Instituto de Física, Universidade de São Paulo, Caixa Postal 66318, 05314-970 São Paulo, São Paulo, Brazil*
[4]*Instituto de Física Gleb Wataghin, Universidade Estadual de Campinas, 13083-970 Campinas, São Paulo, Brazil*

(Received 22 February 2013; accepted 16 April 2013; published online 6 May 2013)

We report momentum transfer cross sections for elastic collisions of low-energy electrons with the HCOOH···$(H_2O)_n$ complexes, with $n = 1, 2$, in liquid phase. The scattering cross sections were computed using the Schwinger multichannel method with pseudopotentials in the static-exchange and static-exchange plus polarization approximations, for energies ranging from 0.5 eV to 6 eV. We considered ten different structures of HCOOH···H_2O and six structures of HCOOH···$(H_2O)_2$ which were generated using classical Monte Carlo simulations of formic acid in aqueous solution at normal conditions of temperature and pressure. The aim of this work is to investigate the influence of microsolvation on the π^* shape resonance of formic acid. Previous theoretical and experimental studies reported a π^* shape resonance for HCOOH at around 1.9 eV. This resonance can be either more stable or less stable in comparison to the isolated molecule depending on the complex structure and the water role played in the hydrogen bond interaction. This behavior is explained in terms of (i) the polarization of the formic acid molecule due to the water molecules and (ii) the net charge of the solute. The proton donor or acceptor character of the water molecules in the hydrogen bond is important for understanding the stabilization versus destabilization of the π^* resonances in the complexes. Our results indicate that the surrounding water molecules may affect the lifetime of the π^* resonance and hence the processes driven by this anion state, such as the dissociative electron attachment.
 [http://dx.doi.org/10.1063/1.4803119]

I. INTRODUCTION

The single- and double-strand breaks in DNA caused by low-energy electrons, that are secondary products of the ionizing radiation interacting with living cells, were first pointed out by Boudaïffa *et al.*[1] This work motivated several experimental and theoretical studies on electron collisions with biological molecules[2] and with molecules that serve as prototypes to biological systems.[3] The capture of the secondary electrons, leading to the formation of transient negative ions (resonances), may result in the dissociation of the anion forms. In particular, both σ^* and π^* shape resonances play an important role in this dissociative electron attachment (DEA) process.[4,5] It is worth noting that any effect that can change the position in energy and the lifetime of these resonances may also affect all the processes related to those states, as DEA.

Some experiments on electron scattering by biological systems have been carried out in a condensed environment, as in a thin DNA film.[6] However, most of the calculations and the experiments in electron collisions with molecules considered the gas-phase. Only few theoretical studies on electron-molecule collisions considered condensed phase effects[7–10] and solvation effects,[11–13] which reported some interesting results. In particular the position, and consequently the lifetime, of the resonances (more generally, their complex potential energy surface) are affected by the environment and can change significantly when passing from gas-phase to condensed phase or to solvated/microsolvated systems. In the case of microsolvated systems, Freitas *et al.*[12] calculated elastic cross sections for electron collisions with the $CH_2O···H_2O$ complex and reported that microsolvation stabilizes the π^* shape resonance of the solute, causing a downshift of ∼0.6 eV with respect to the resonance of the isolated molecule, lying at 1 eV. In all the addressed $CH_2O···H_2O$ complexes the water molecule played the role of proton donor.

The goal of this paper is to investigate the influence of microsolvation in the π^* shape resonance of formic acid, considering one and two surrounding water molecules. Formic acid is an interesting solute molecule because the isolated molecule has a well known π^* resonance at around 1.9 eV, as reported by several different experimental and theoretical methodologies.[14–24] Formic acid has two stable isomers, namely, *trans*-HCOOH and *cis*-HCOOH. The π^* resonance of the two isomers is located at the same energy.[14] The present study goes beyond the work of Ref. 12. Here we consider one

a)Electronic mail: bettega@fisica.ufpr.br

and two water molecules from the aqueous solution. We analyze the role of the water molecules as proton donor and/or proton acceptor in the stabilization/destabilization of the π^* resonance of the solute, and discuss some aspects that would affect the lifetime of this shape resonance, such as the interaction polarizability and the net charge of the solute.

In this paper we present momentum transfer cross sections for elastic collisions of electrons with the complexes composed by one molecule of formic acid and one or two molecules of water. The cross sections were computed with the Schwinger multichannel (SMC) method implemented with pseudopotentials in the static-exchange (SE) and in the static-exchange-polarization (SEP) approximations, for energies ranging from 0.5 eV to 6 eV. The solute and the water molecules are bound together by hydrogen bonds. We considered 16 (ten for $n = 1$ and six for $n = 2$) different structures for the complexes which were obtained from classical Monte Carlo simulation of HCOOH in liquid water environment at room temperature and pressure.[25] After the simulation, some statistically representative hydrogen-bonded complexes were sampled for electron collision targets. The structures considered in this work are shown in Figs. 1 and 2 for the HCOOH$\cdots$H$_2$O complexes, labeled from

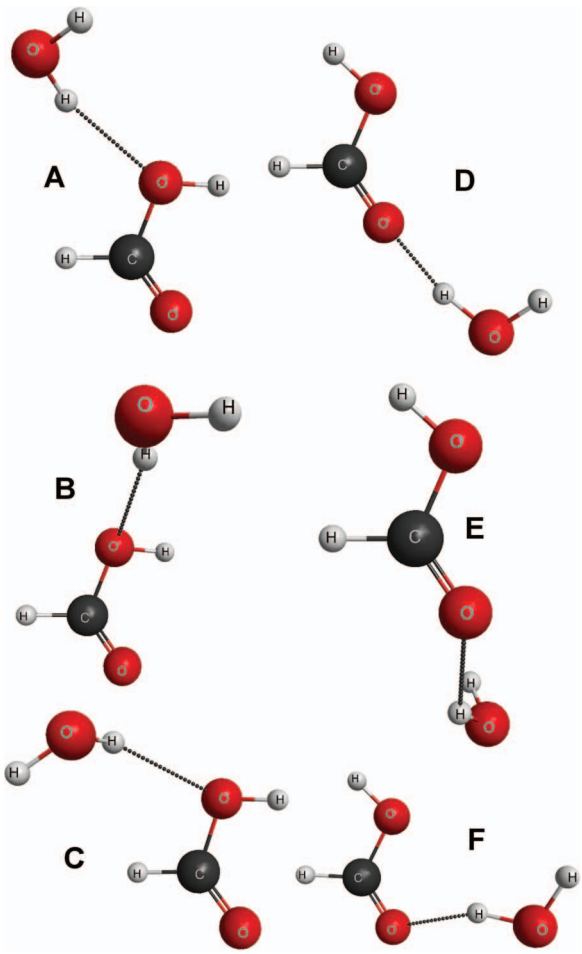

FIG. 1. Geometrical structures of six possible structures of the complexes (hydrogen-bonded pairs HCOOH$\cdots$H$_2$O) named **A** to **F**. Complexes **A** to **C** were build with the *trans* isomer of formic acid and the complexes **D** to **F** with the *cis* isomer of formic acid. These plots were generated using MacMolPlt.[26]

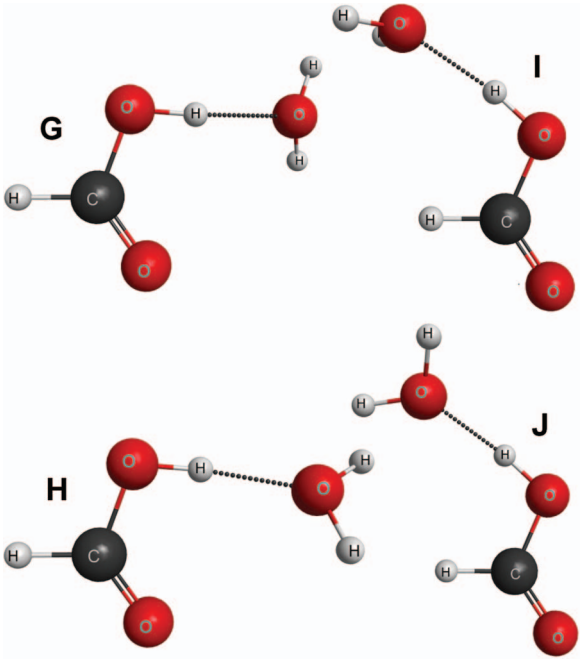

FIG. 2. Geometrical structures of four possible structures of the complexes (hydrogen-bonded pairs HCOOH$\cdots$H$_2$O) named **G** to **J**. Complexes **G** and **H** were build with the *trans* isomer of formic acid and the complexes **I** and **J** with the *cis* isomer of formic acid. These plots were generated using MacMolPlt.[26]

A to **J**, and in Fig. 3 for the HCOOH$\cdots$(H$_2$O)$_2$ complexes, labeled from **K** to **P**. The complexes **A**, **B**, **C**, **G**, **H**, **K**, **L**, and **M** were generated considering the *trans*-HCOOH isomer of HCOOH, and the complexes **D**, **E**, **F**, **I**, **J**, **N**, **O**, and **P** were generated considering the *cis*-HCOOH isomer. All the molecular plots shown in Figs. 1–3 were generated using MacMolPlt program.[26]

The remainder of this paper is organized as follows. In Sec. II we present the theoretical method and the computational procedures used in the present calculations. Section III presents our results, which are discussed in Sec. IV. The conclusions of this work are presented in Sec. V.

II. COMPUTATIONAL PROCEDURES

A. Liquid simulation

To generate the structures of the HCOOH$\cdots$(H$_2$O)$_n$ ($n = 1, 2$) complexes in the liquid phase, we performed classical computer simulations of the *trans* and *cis* formic acid isomers separately surrounded by 1000 water molecules under normal conditions of temperature and pressure (T = 298.15 K and P = 1 atm) in the NPT ensemble. We used the Monte Carlo (MC) method with the Metropolis sampling technique and the classical force field comprising the Lennard-Jones and Coulomb potentials, as described before,[25] with the DICE program.[27] The water molecules were described by the SPC/E model.[28] The geometries of formic acid isomers were kept rigid during the simulation and were obtained by optimization in the quantum mechanics calculation using second order perturbation method (MP2)[29,30] and the aug-cc-pVDZ[31] basis function using the GAUSSIAN program.[32] The interactions of

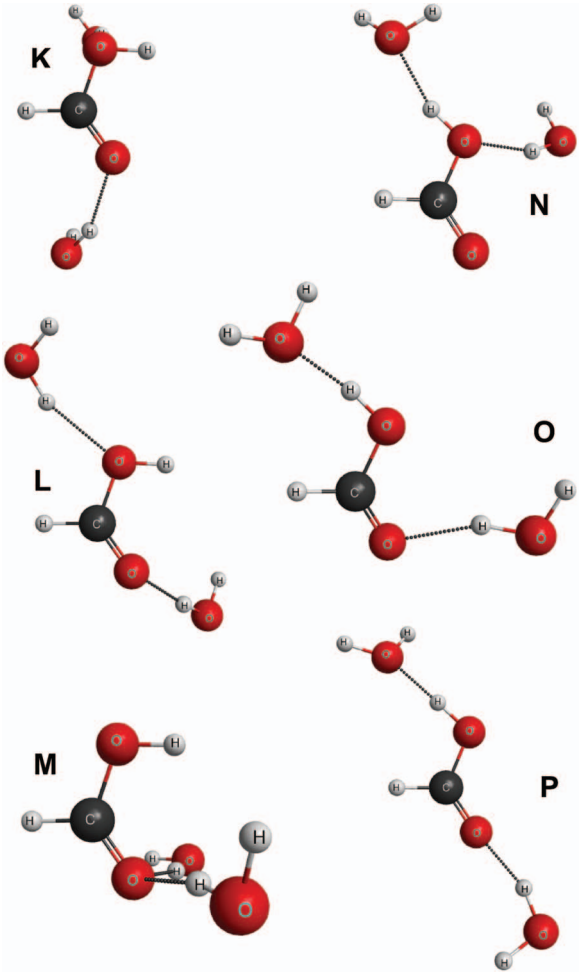

FIG. 3. Geometrical structures of six possible structures of the complexes (hydrogen-bonded pairs $HCOOH\cdots(H_2O)_2$) named **K** to **P**. Complexes **K** to **M** were build with the *trans* isomer of formic acid and the complexes **N** to **P** with the *cis* isomer of formic acid. These plots were generated using MacMolPlt.[26]

the formic acid were described by the OPLS (optimized potential of liquid systems) force field.[33] However, the atomic charges were modified to include the electronic polarization effect due to the presence of the solvent. These charges were generated by the fitting of the electrostatic potential of the formic acid in aqueous solution using the ChelpG (charges from electrostatic potentials using a grid) procedure.[34] The electrostatic potential, the charge distribution, and the dipole moment were obtained from a quantum mechanics calculation using MP2/aug-cc-pVDZ and considering the aqueous environment as a polarizable continuum model (PCM).[35] The calculated dipole moment for the polarized formic acid in water is 1.93 D and 5.19 D for its *trans* and *cis* isomers, respectively. These values show an increase in the dipole moment of approximately 36% for the *trans*-HCOOH and 33% for the *cis*-HCOOH compared to the formic acid in gas-phase (1.42 D and 3.89 D, respectively). This polarization process was used before and proved to be adequate in the description of the electronic polarization of the solute in aqueous solution.[36,37] The geometries and the force field parameters for the formic acid and the water molecule are presented in Table I.

TABLE I. Cartesian coordinates x and y (in Å) for the planar molecules: formic acid and water, and the force field parameters: atomic charge, q (in e), and the Lennard-Jones parameters, ϵ (in kcal/mol) and σ (in Å).

Atom	x	y	q	ϵ	σ
cis-HCOOH					
C	−0.0075	−0.0364	0.6805	0.105	3.750
O	1.3574	0.0012	−0.6011	0.170	3.000
H	1.6432	0.9282	0.4669	0.000	0.000
O	−0.6226	−1.0770	−0.5681	0.210	2.960
H	−0.4805	0.9670	0.0218	0.000	0.000
trans-HCOOH					
C	−0.0180	−0.0546	0.6776	0.105	3.750
O	1.3371	0.0399	−0.6266	0.170	3.000
H	1.6764	−0.8741	0.4912	0.000	0.000
O	−0.6467	−1.0947	−0.5999	0.210	2.960
H	−0.4589	0.9564	0.0577	0.000	0.000
Water SPC/E					
O	0.0000	0.0000	−0.8476	0.155	3.165
H	0.5774	0.8165	0.4238	0.000	0.000
H	0.5774	−0.8165	0.4238	0.000	0.000

The simulation was performed in two stages, the thermalization with 6×10^7 MC step and the equilibrium with 1.2×10^8 MC step. After thermodynamic equilibration 9×10^4 configurations were saved and the distribution of water molecules around the formic acid were analyzed using the radial distribution function between the oxygen atoms of formic acid and water molecules and the characterization of the formic acid-water hydrogen bonds (HBs). As described before,[25,37] the HBs were defined using the geometric and energetic criteria: a distance between the oxygen atoms of formic acid and of water molecules, $R_{OO} \leq 3.2$ Å (value of the first minimum in the $G_{OO}(r)$), an angle between O and OH, $\theta(O\cdots OH) \leq 35^\circ$, and a binding energy (calculated by the classical force field) $E_{ij} \leq -0.01$ kcal/mol. This energy criterion is used only to guarantee that the water molecule is hydrogen bonded to the formic acid.

B. Cross sections calculations

The SMC method and its implementation with pseudopotentials have been described in detail elsewhere.[38–40] Here we only outline its main aspects. The working expression for the scattering amplitude in the body-fixed frame is

$$f^{SMC}(\vec{k}_f, \vec{k}_i) = -\frac{1}{2\pi}\sum_{m,n}\langle S_{\vec{k}_f}|V|\chi_m\rangle(d^{-1})_{mn}\langle\chi_n|V|S_{\vec{k}_i}\rangle, \tag{1}$$

where

$$d_{mn} = \langle\chi_m|A^{(+)}|\chi_n\rangle \tag{2}$$

and

$$A^{(+)} = \frac{1}{2}(PV + VP) - VG_P^{(+)}V + \frac{\hat{H}}{N+1} - \frac{1}{2}(\hat{H}P + P\hat{H}). \tag{3}$$

In the expressions above, $\{\chi_m\}$ are $(N+1)$-electron trial configuration-state functions (CSFs), spin-adapted products

TABLE II. Uncontracted Cartesian Gaussian functions used for carbon and oxygen.

Type	Carbon Exponent	Oxygen Exponent
s	12.49628	16.05878
s	2.470286	5.920242
s	0.614028	1.034907
s	0.184028	0.316843
s	0.039982	0.065203
p	4.911060	10.14120
p	1.339766	2.782999
p	0.405869	0.841004
p	0.117446	0.232939
d	0.603592	0.756793
d	0.156753	0.180759

of target states with one-particle scattering orbitals. $S_{\vec{k}_{i(f)}}$ is an eigenstate of the unperturbed Hamiltonian H_0, given by the product of a target state and a plane wave with momentum $\vec{k}_{i(f)}$; V is the interaction potential between the incident electron and the target; $\hat{H} \equiv E - H$, where E is the collision energy and $H = H_0 + V$ is the scattering Hamiltonian; P is a projection operator onto the open-channel target space and $G_P^{(+)}$ is the free-particle Green's function projected on the P-space.

Bound-state and scattering calculations were performed for the 16 structures composed of one formic acid molecule and one or two water molecules as shown in Figs. 1–3. The 1*s* core electrons of carbon and oxygen were replaced by the *norm-conserving* pseudopotentials of Bachelet, Hamann, and Schlüter.[41] The Cartesian Gaussian basis sets used to represent the single-particle functions are given in Table II, and were generated according to Ref. 42. For the hydrogen atoms we employed the Dunning basis set[43] augmented with one uncontracted *p*-type function with exponent 0.75, as shown in Table III. Additional functions at the center of mass were also used, as shown in Table III. All *d*-type functions used are five-component in order to avoid numerical linear dependency.

As mentioned before scattering calculations were carried out in the SE and in the SEP approximations. In the former, the $(N + 1)$-electron basis set is constructed as

$$|\chi_n\rangle = \mathcal{A}|\Phi_1\rangle \otimes |\varphi_n\rangle,$$

TABLE III. Cartesian Gaussian functions used for hydrogen and the center of mass.

	Hydrogen		Center of mass	
Type	Exponent	Coefficient	Exponent	Coefficient
s	13.3615	0.130844	0.04	1.0
	2.0133	0.921539	0.01	1.0
	0.4538	1.0		
	0.1233	1.0		
p	0.7500	1.0	0.08	1.0
			0.02	1.0

where $|\Phi_1\rangle$ is the Hartree-Fock (HF) target ground state, $|\varphi_n\rangle$ is a single-particle orbital, and $\mathcal{A}$ is the antisymmetrizer. In the SEP approximation, the above trial set is augmented with configuration state functions (CSF) constructed as

$$|\chi_{mn}\rangle = \mathcal{A}|\Phi_m\rangle \otimes |\varphi_n\rangle,$$

where $|\Phi_m\rangle$ are N-electron Slater determinants obtained by single excitations from the occupied (hole) orbitals to a set of unoccupied (particle) orbitals. Modified virtual orbitals (MVO)[44] generated for a +4 cationic operator were employed to represent the particle and scattering orbitals in the SEP calculations.

For the HCOOH···H_2O complexes we considered the 13 valence occupied orbitals as hole orbitals and the 22 first MVO as particle and scattering orbitals. For the HCOOH···$(H_2O)_2$ complexes we considered the 13 outermost occupied orbitals as hole orbitals, and the 22 first MVO as particle and scattering orbitals. Though only doublet CSFs were kept in the scattering calculations, as described in Ref. 45, both singlet- and triplet-coupled target excitations were taken into account in the calculations. We thus obtained 6419 (doublets) CSFs for each HCOOH···H_2O complex structure and 6454 CSFs for each HCOOH···$(H_2O)_2$ complex structure.

All the complexes considered here have a permanent electric dipole moment. The long range character of the dipole potential requires the use of the standard Born closure to improve the cross sections. However, this potential only affects the background scattering and does not change the location of the resonances. Since our main interest here is the description of the π^* shape resonance of the complexes, we chose to present only the momentum transfer cross section (MTCS), which is only slightly affected by the dipole potential (mainly at low energies).

We have also calculated the MTCS for the *trans*-HCOOH and *cis*-HCOOH isomers at the same geometries employed in the liquid simulation. The resulting π^* anion states for the *trans* and *cis* isomers are located at the same energy, namely, 3.5 eV (in agreement with the previous study[20]), in the SE approximation, and at 1.9 eV (in agreement with previous studies[14–21]), in the SEP approximation.

III. RESULTS

The MC simulation of the infinite dilution of formic acid in water (1 HCOOH + 1000 H_2O) at normal conditions of temperature and pressure (T = 298.15 K and P = 1 atm) provides an average density of 1.021 ± 0.008 g/cm^3 and an average size length of the simulation box of 30.8 Å. With the configurations generated in these simulations the distribution of water molecules around the formic acid were analyzed using the radial distribution function between the carbonyl oxygen (=O) of formic acid and the oxygen of the water molecules, $G_{OO}(r)$, and the characterization of the formic acid-water hydrogen bonds, where both molecules played the role of proton donor and proton acceptor. In Fig. 4 this $G_{OO}(r)$ is shown. It is easy to identify at least three peaks that characterize the hydrogen bonds microsolvation shell of the formic acid up to 3.2 Å, the first solvation shell from 3.2 to 5.5 Å and the

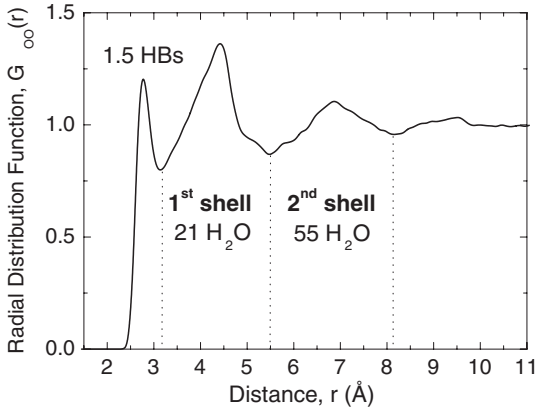

FIG. 4. Radial distribution function between the carbonyl oxygen (=O) of formic acid and the oxygen of the water molecules, $G_{OO}(r)$. The vertical lines highlight the peaks that characterize the hydrogen bonds microsolvation, the first and second solvation shells of the formic acid in aqueous solution.

second solvation shell from 5.5 to 8.2 Å. The integration of these peaks in spherical shells gives the number of water molecules that compose the solvation shells around the carbonyl oxygen of the formic acid. Performing the same analysis of the radial distribution functions between the carbon and the hydroxyl oxygen (–O) of the formic acid and the oxygen of water molecules, we found in average 3 water molecules in the HB microsolvation, 21 in the first, and 55 in the second solvation shells. Using the geometric and energetic criteria to have a better definition of the hydrogen bonds, we identified about 1.5 water molecules bound to the carbonyl oxygen, 0.5 water molecules bound to the hydroxyl oxygen, and 1.0 water molecule bound to the hydroxyl hydrogen. This gives a total of 3 HBs on average, where in 2 of them the water molecules play the role of proton donor and in 1 of proton acceptor. We also identified that the sampled configurations have 1–4 HBs, where 100% of them have at least 1 HB, around 97% have at least 2 HBs, 70% at least 3 HBs, and 20% at least 4 HBs. Therefore, we decided to study the most frequent possibility of complexes with 1 and 2 HBs. Within a wide variety of sampled configurations, we selected ten complexes with 1 HB (**A** to **J** complexes in Figs. 1 and 2) and six with 2 HBs (**K** to **P** complexes in Fig. 3). These complexes were chosen due to the large structural difference between them, which represent a wide diversity of structures thermodynamically accessible in the solution. Therefore, with these 16 complexes we attempt to understand the influence of microsolvation on the π^* resonance of the solute and also the role of the proton donor and proton acceptor played by the water molecules in the hydrogen bond(s) in the stabilization/destabilization of this resonance.

In Fig. 5 we show the MTCS for the six HCOOH···H_2O complexes **A** to **F** (according Fig. 1), where the water molecule plays the role of proton donor, in the SE and SEP approximations. There is, for each complex, one structure at around 3 eV in the SE MTCS, which represents the π^* shape resonance of the solute. This resonance is more stable in the complexes, with a downshift of ∼0.5 eV with respect to the SE result of 3.5 eV for the isolated molecule. The same behavior is seen in the SEP calculations, which locate the

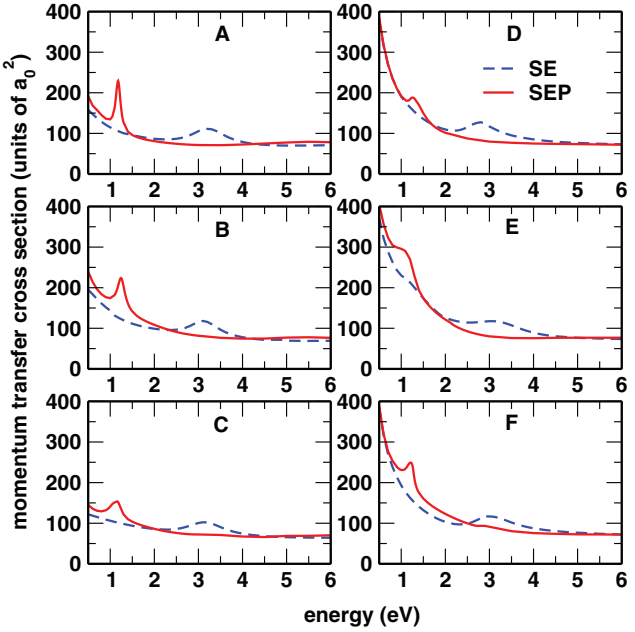

FIG. 5. Momentum transfer cross sections in the SE and SEP approaches for the six complexes **A** to **F**. See text for discussion.

π^* shape resonance of the complexes at around 1.3 eV and ∼0.6 eV lower than the π^* resonance of the isolated formic acid molecule, which is located at around 1.9 eV. Therefore, we observe a stabilization (augmenting the lifetime) of the resonance, when moving from the formic acid calculations in the gas-phase to the HCOOH···H_2O complexes calculations, which consider microsolvation. These conclusions are also supported by the results reported by Baccarelli *et al.*[11] and by Freitas *et al.*[12]

Figure 6 shows the MTCS for the four HCOOH···H_2O complexes **G** to **J** (according Fig. 2), now with the water

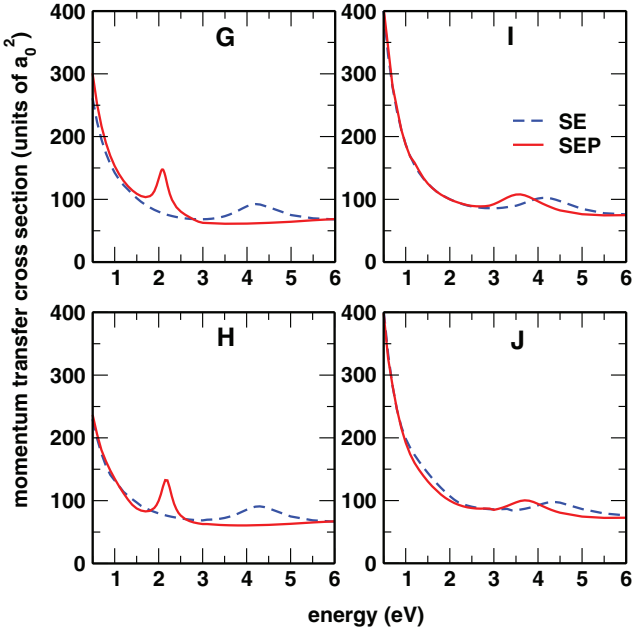

FIG. 6. Momentum transfer cross sections in the SE and SEP approaches for the four complexes **G** to **J**. See text for discussion.

molecule as a proton acceptor, in the SE and SEP approximations. For each complex, there is one structure at around 4.5 eV in the SE MTCS. These results show that in this case there is the destabilization of the resonance, located at about 1 eV above the resonance of the isolated molecule. In the SEP approximation for the complexes **G** and **H**, the resonance is located at around 2.2 eV, which is about 0.3 eV above the resonance of the isolated molecule, while for the complexes **I** and **J** it is located at around 3.6 eV, at about of 1.7 eV above the resonance of the isolated molecule. These results show that the destabilization of the resonance occurs if the water molecule plays the role of proton acceptor.

In Fig. 7 we show the MTCSs obtained in the SE and SEP approximations for the six HCOOH$\cdots$$(H_2O)_2$ complexes, namely, **K** to **P**. Considering the SE results for the complexes **K**, **L**, and **M**, the peaks lie between 2.5 eV and 2.7 eV which corresponds to a downshift of ∼1 eV in comparison with the SE results of the isolated formic acid molecule. However, for the complexes **N**, **O**, and **P**, the resonances move to a higher energy in comparison to the π^* resonance of formic acid, being located at around 3.7 eV. This corresponds to a shift of ∼0.2 eV to higher energy compared to the SE results of the formic acid molecule. A similar behavior occurs in the SEP calculations where for the complexes **K**, **L**, and **M** a downshift occurs, and the resonances lie between 1.5 eV and 1.7 eV. For the complexes **N**, **O**, and **P** the resonances lie between 2.2 eV and 2.3 eV, which is ∼0.3 eV higher than the isolated formic acid molecule. Also for the $n = 2$ case, either stabilization (complexes **K**, **L**, and **M**) and destabilization (complexes **N**, **O**, and **P**) of the π^* shape resonance of the solute is observed. All the values for the energy of the π^* resonance (E_r) obtained with the SEP calculations for the 16 structures, **A** to **P**, are presented in Table IV.

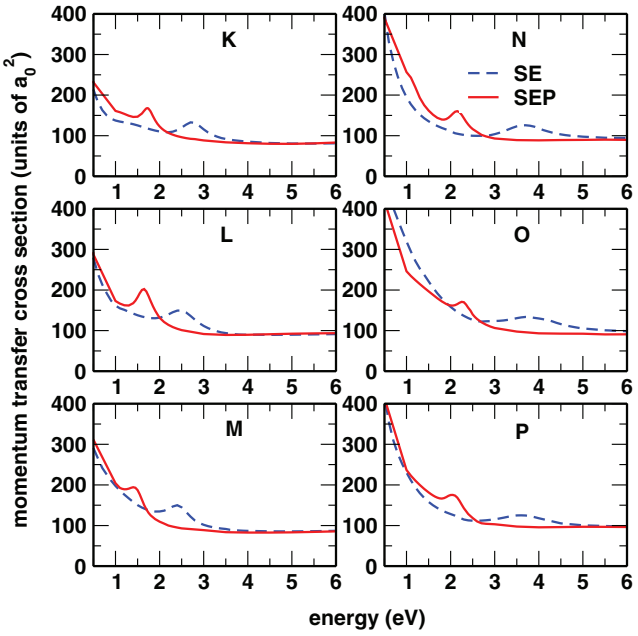

FIG. 7. Momentum transfer cross sections in the SE and SEP approaches for the six complexes **K** to **P**. See text for discussion.

IV. DISCUSSION

The experimental values for the dipole moments of H_2O and *trans*-HCOOH are 1.85 D and 1.41 D,[46] respectively. We have not found in the literature the experimental value for the

TABLE IV. Dipole moment, μ (in D), vertical attachment energy, VAE (in units of eV), dipole moment of the formic acid in aqueous solution, $\mu(\text{HCOOH})_{aq}$, induce dipole moment due to the aqueous solution, $\Delta\mu$, the net charge sign, q_{net}, and the energy of the resonance peak using the SEP approximation, E_r. In brackets the experimental values are presented for the dipole moment[46] and the energy of the resonance.[14–24]

	μ	VAE	$\mu(\text{HCOOH})_{aq}$	$\Delta\mu$	q_{net}	E_r
H_2O	1.81 [1.85]	5.26				[10.0] (σ^*)
trans-HCOOH	1.42 [1.41]	3.59				1.9 [1.9] (π^*)
cis-HCOOH	3.89	3.59				1.9 (π^*)
A	1.85	3.18	1.94	0.53 (36%)	+	1.2 (π^*)
B	1.49	3.29	1.93	0.52 (36%)	+	1.2 (π^*)
C	1.73	3.32	1.94	0.53 (36%)	+	1.2 (π^*)
D	6.29	2.75	5.45	1.56 (40%)	+	1.2 (π^*)
E	5.92	3.08	5.28	1.39 (36%)	+	1.1 (π^*)
F	6.06	2.99	5.25	1.36 (35%)	+	1.3 (π^*)
G	3.05	4.19	1.95	0.53 (37%)	−	2.1 (π^*)
H	2.65	4.18	1.96	0.54 (38%)	−	2.2 (π^*)
I	6.52	3.80	5.33	1.44 (37%)	−	3.5 (π^*)
J	6.78	3.85	5.33	1.44 (37%)	−	3.7 (π^*)
K	4.43	2.74	2.07	0.65 (46%)	+	1.7 (π^*)
L	3.08	2.37	2.00	0.58 (41%)	+	1.6 (π^*)
M	4.40	2.09	1.95	0.53 (37%)	+	1.5 (π^*)
N	8.00	3.70	5.37	1.48 (38%)	−	2.2 (π^*)
O	9.25	3.84	5.31	1.41 (36%)	−	2.3 (π^*)
P	9.35	3.61	5.41	1.52 (39%)	−	2.1 (π^*)

dipole moment of *cis*-HCOOH. There is a very good agreement between our calculated results (1.81 and 1.42 D with MP2/aug-cc-pVDZ, respectively) and the experimental values, as shown in Table IV. In this table the permanent electric dipole moments of all complexes are also shown. Note that the complexes **A** to **C** and **G** and **H**, and **K** to **M** have lower dipole moments (from 1.49 to 4.43 D) due to the presence of the *trans* form of the formic acid and the complexes **D** to **F**, **I** and **J**, and **N** to **P** have higher dipole moments (from 5.92 to 9.35 D) due to the presence of the *cis* form. This difference in the permanent dipole moment of the complexes is related to the difference in the increasing slope of the cross section at very-low energy region that can be seen in Figures 5–7. Therefore, complexes with a lower dipole moment present a slow increase in the cross section as the energy decreases and complexes with a higher dipole moment present strong increase.

Complexes **A** to **F** present a downshift on the resonance position of approximately 0.5 eV and 0.6 eV in the SE and SEP calculations, respectively, with respect to the resonance of the formic acid molecule in gas-phase (3.5 eV in SE and 1.9 eV in SEP). Similar results were previously reported in the literature for electron collisions with solvated glycine, where the solvation was described by a continuum medium (using the polarizable continuum model),[7] for electron collisions with the $CH_2O\cdots H_2O$ complexes,[12] and for electron attachment to CF_2Cl_2 and CF_3Cl molecules in a cluster environment.[13] On the other hand, the resonance of the complexes **G** to **J** are located above of the resonance of the isolated molecule. For these four complexes, the resonance location, computed in the SE approximation, is at about 1 eV above the resonance of the isolated molecule. In the SEP approximation the resonance position for the complexes **G** to **J** is above the resonance of the gas-phase position about 0.3 eV (**G** and **H**) and 1.7 eV (**I** and **J**), respectively. For the $n = 1$ case stabilization of the anion state occurs if the water is proton donor in the hydrogen bond interaction; if the water plays a role of proton acceptor, the anion state destabilizes.

In electron collision with biologically relevant systems, Martin *et al.*[4] pointed out the competition between polarization (due to the environment), that may contribute to the stabilization of the resonances, and negatively charged sites, that can lead to the destabilization of the resonances. In order to investigate what causes the stabilization/destabilization of the π^* resonance of the solute in the complexes, we have performed a systematic analysis of some quantities obtained from bound state calculations: the vertical attachment energy, the solute polarization, and the net charge in the solute, which are presented in Table IV. First, we computed the vertical attachment energies (VAE) for the isolated *trans*- and *cis*-HCOOH and for the complexes **A** to **P** in a Hartree-Fock calculation with the DZV basis set using the computational package GAMESS.[47] The calculated values for the VAE are the negative of the vertical electron affinity which corresponds, by Koopmans theorem, to the canonical eigenvalues of the Fock operator of the unoccupied orbitals. Table IV shows that for the *trans* complexes **A** to **C**, and **K** to **M** the VAE value is smaller than the VAE value of the isolated *trans*-HCOOH. The same is true for the VAE value of the *cis* complexes **D**, **E**, and **F** in comparison with the VAE value of the isolated *cis*-HCOOH. However, for the complexes **N**, **O**, and **P** the VAE is larger than for the isolated *cis*-HCOOH. This is also true for the *trans* complexes **G** and **H**, and *cis* complexes **I** and **J**, which have VAE larger than the corresponding gas-phase isomers. Since the VAE value can be related to the position in energy of the π^* shape resonance,[48] this is a first indication that in the complexes **A** to **F** and **K** to **M** the π^* resonance should stabilize and for the complexes **G** to **J** and **N** to **P** the π^* resonance should destabilize. The π^* character of the orbitals responsible for the resonances was investigated by the inspection of the lowest unoccupied orbital (LUMO) of the complexes obtained in a bound state calculation (as described above). For each complex, the resulting LUMO is mostly localized on the solute, with a small contribution from the solvent for some complexes, and is spatially very similar to the LUMO of the isolated formic acid,[49] having a π^* character, as shown in Figs. 8–10.

The second aspect we have investigated is the polarization of the formic acid molecule due to the surrounding water molecules. The quantity to describe this property is the difference of the dipole moment of the solute in gas-phase and in aqueous solution,[50] $\Delta\mu = \mu(\text{HCOOH})_{aq} - \mu(\text{HCOOH})$. The values of the dipole moment were obtained using MP2 calculation with the aug-cc-PVDZ basis set. The dipole moment of the solute in aqueous solution, $\mu(\text{HCOOH})_{aq}$, was calculated considering only the HCOOH explicitly and the aqueous environment described in two regions: the $(H_2O)_n$ (with $n = 1$, 2) presented in the cluster as point charges and the remaining bulk water as polarizable continuum model (PCM).[51,52] The calculated $\mu(\text{HCOOH})_{aq}$ for the complexes are also shown in Table IV. These values for the *trans* complexes vary from 1.93 to 2.07 D, which show a polarization of 36% to 46% (approximately 0.5–0.7 D) compared to the isolated formic acid, where $\mu(trans\text{-HCOOH}) = 1.42$ D. For the *cis* complexes $\mu(\text{HCOOH})_{aq}$ vary from 5.25 to 5.45 D, which show a polarization of 35%–40% (approximately 1.4–1.6 D) compared to the isolated formic acid, where $\mu(cis\text{-HCOOH}) = 3.89$ D. Therefore, all complexes show a polarization of around 40% and this should stabilize the π^* resonance energy peak, E_r. Therefore, apparently there is no direct correlation between the solute polarization and the stabilization/destabilization of the π^* resonance.

We then investigated the electrostatic effects of the complexes by looking at the net charge of the solute considering the complexes with one and two water molecules. Hartree-Fock calculations using 6-31G(*d*) basis set and MP2 calculations using aug-cc-pVDZ basis set were performed for the complexes, where the Mulliken population analysis was carried out and the net charge of each atom of the solute was summed. As the numerical results of the Mulliken population is very sensitive to the basis set and other calculation details,[53,54] we only considered the sign of the solute net charge. Since the resonant orbital in the complexes is mostly localized on the solute (according to Figs. 8–10), a positive net charge represents a more attractive electrostatic static potential seen by the incoming electron, which would lead to the stabilization of the π^* shape resonance. Otherwise, for a negatively charged solute, the incoming electron would feel

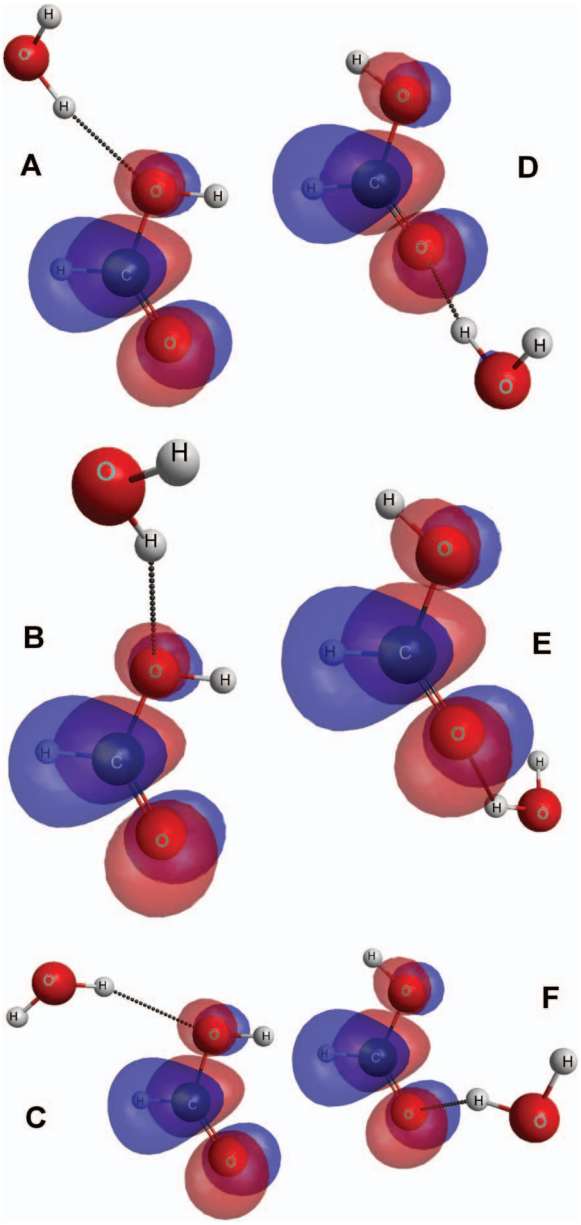

FIG. 8. Plots for the LUMO of the complexes **A** to **F**. See text for discussion. These plots were generated using MacMolPlt.[26]

a less attractive static potential, leading to the destabilization of the resonance. The signs of the net charges are shown in Table IV for all the complexes. For the six HCOOH$\cdots$H$_2$O complexes where the water is proton donor the net charge of the solute is positive and would also explain the stabilization of the π^* resonance. For the remaining four HCOOH$\cdots$H$_2$O complexes, where the water plays the role of proton acceptor, the net charge of the solute is negative, which explains the destabilization of the anion state. In the case of the HCOOH$\cdots$(H$_2$O)$_2$ complexes, there is a positive net charge in the solute for the **K**, **L**, and **M** complexes, which would also lead to the stabilization of the resonance. However, for the complexes **N**, **O**, and **P** the net charge in the solute is negative, and would explain the destabilization of the resonance. If we consider only the electrostatic effects due to the net charge, we find qualitative agreement with our calculated scattering

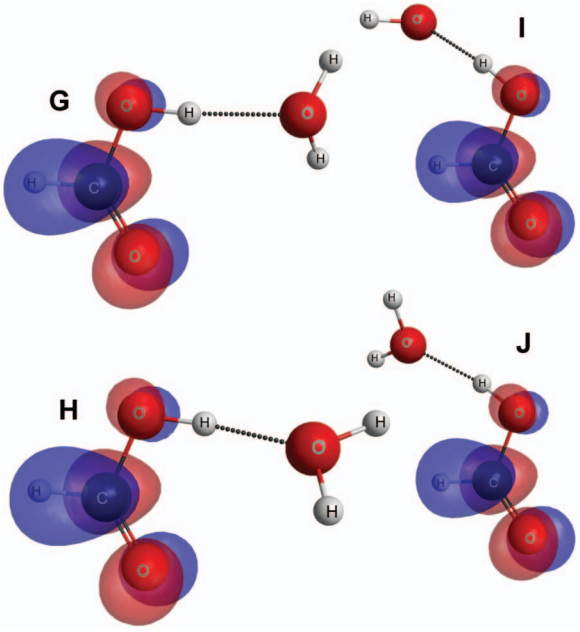

FIG. 9. Plots for the LUMO of the complexes **G** to **J**. See text for discussion. These plots were generated using MacMolPlt.[26]

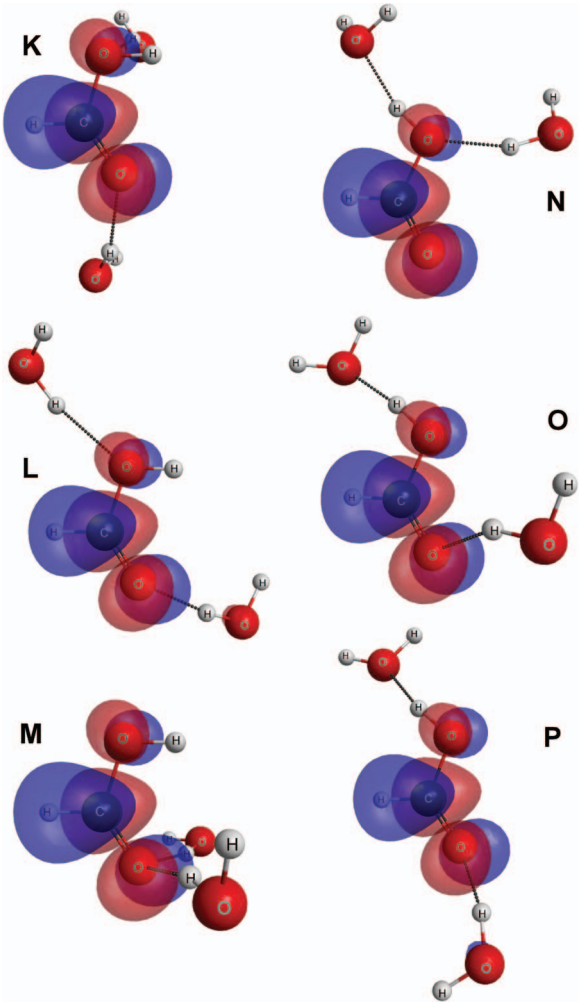

FIG. 10. Plots for the LUMO of the complexes **K** to **P**. See text for discussion. These plots were generated using MacMolPlt.[26]

cross sections. When the solute is positively charged the resonance stabilizes and for systems with a negative charge in the solute, the resonance destabilizes. Again, the presence of at least one water as proton acceptor leads to the destabilization of the resonance.

In the case of the complexes **A** to **F** and **K** to **L**, both the polarization (due to the surrounding water molecules) and the net charge in the solute may contribute to the stabilization of the π^* resonance. However, for the complexes **G** to **J** and **N** to **P**, the polarization indicates stabilization while the net charge leads to the destabilization of the resonance. The final answer about stabilization/destabilization of the resonance is given by the cross sections obtained in the scattering calculations, as shown in Figs. 5–7.

For the $HCOOH\cdots H_2O$ complexes **A** to **F**, the water molecule is a proton donor in the hydrogen bond. The same is true for the complexes **K** to **M**, where both water molecules are proton donor in the hydrogen bonds. In these cases, the role played by the water molecule(s) in the hydrogen bond(s) is responsible for the positive net charge in the solute. For the complexes **G** to **J** the water is proton acceptor and for the complexes **N** to **P**, however, one water molecule is proton donor in the hydrogen bond and the other is proton acceptor. For the $n = 2$ case, the final result is obtained by the interplay and gives a net of negative charge of the solute. Again, the final answer about stabilization/destabilization of the resonance is provided by the scattering calculations.

V. SUMMARY AND CONCLUSIONS

In this work, we reported elastic MTCS for the $HCOOH\cdots(H_2O)_n$ complex, with $n = 1, 2$ in liquid phase. We considered 16 different structures which were generated by classical Monte Carlo simulations with temperature and pressure effects. The cross sections calculations indicate that the π^* resonance of the isolated formic acid molecule, which is located at around 1.9 eV, stabilizes when the calculations are performed for the hydrogen bonded complexes with one water molecule as proton donor, and destabilizes if the water plays the role of proton acceptor ($n = 1$ case). For the case of two water molecules, $n = 2$, when both water molecules are proton-donor in the hydrogen bonds, the anion state stabilizes but when one water molecule is proton-donor hydrogen bond and the other is proton-acceptor, it destabilizes. The low-lying LUMOs of the complexes are mostly localized on the solute (with a small contribution from the solvent for some structures) and show the same π^* character of the LUMO of the isolated formic acid molecule. We have explored two effects that may affect the π^* shape resonance, namely, the solute polarization and the net charge of the solute, and also the possible competition between them. Both polarization and positive net charge may contribute to the stabilization of the anion state; a negative net charge may cause destabilization of the π^* resonance. The change from gas to condensed-phase and the effects induced by the microsolvation in electron-molecule calculations are important steps in the understanding of how the environment may affect processes in DNA driven by electron collisions and anion states. The results of this paper show that microsolvation effects can change the position in energy of a π^* shape resonance of a small solute in comparison with the system in the gas-phase (more generally, it affects the resonance lifetime and the complex potential energy curve of the negative ion). We believe that the present study establishes a basis for understanding the effects induced by the microsolvation in a transient negative ion and for future investigations on electron collisions with microsolvated systems.

ACKNOWLEDGMENTS

K.C., M.T.N.V., M.A.P.L., and S.C. acknowledge support from CNPq, CAPES, and FAPESP. M.H.F.B. acknowledges support from CNPq and FINEP (under project CT-Infra). T.C.F. and M.H.F.B acknowledge computational support from Professor Carlos M. de Carvalho at LFTC-DFis-UFPR and at LCPAD-UFPR. The authors also acknowledge computational support from CENAPAD-SP.

[1] B. Boudaïffa, P. Cloutier, D. Hunting, M. A. Huels, and L. Sanche, Science **287**, 1658 (2000).
[2] See, for example, G. Hanel, B. Gstir, S. Denifl, P. Scheier, M. Probst, B. Farizon, M. Farizon, E. Illenberger, and T. D. Märk, Phys. Rev. Lett. **90**, 188104 (2003); S. Denifl, S. Ptasinska, M. Cingel, S. Matejcik, P. Scheier, and T. D. Märk, Chem. Phys. Lett. **377**, 74 (2003); H. Abdoul-Carime, S. Gohlke, and E. Illenberger, Phys. Rev. Lett. **92**, 168103 (2004).
[3] See, for instance, C. Winstead and V. McKoy, J. Chem. Phys. **125**, 074302 (2006); **125**, 244302 (2006); C. Winstead, V. McKoy, and S. d'A. Sanchez, *ibid.* **127**, 085105 (2007); J. D. Gorfinkel, L. G. Caron, and L. Sanche, J. Phys. B: At. Mol. Opt. Phys. **39**, 975 (2006); E. M. de Oliveira, M. A. P. Lima, M. H. F. Bettega, S. d'A. Sanchez, R. F. da Costa, and M. T. do N. Varella, J. Chem. Phys. **132**, 204301 (2010), and references therein.
[4] F. Martin, P. D. Burrow, Z. Cai, P. Cloutier, D. Hunting, and L. Sanche, Phys. Rev. Lett. **93**, 068101 (2004).
[5] A. M. Scheer, K. Aflatooni, G. A. Gallup, and P. D. Burrow, Phys. Rev. Lett. **92**, 068102 (2004).
[6] L. Sanche, Eur. Phys. J. D **35**, 367 (2005).
[7] F. A. Gianturco, R. R. Luchese, J. Langer, I. Martin, M. Stano, G. Karwasz, and E. Illenberg, Eur. Phys. J. D **35**, 417 (2005).
[8] T. C. Freitas, S. A. Sanchez, M. T. do N. Varella, and M. H. F. Bettega, Phys. Rev. A **84**, 062714 (2011).
[9] L. Caron, D. Bouchiha, J. D. Gorfinkiel, and L. Sanche, Phys. Rev. A **76**, 032716 (2007).
[10] S. Caprasecca, J. D. Gorfinkel, D. Bouchiha, and L. Caron, J. Phys. B **42**, 095205 (2009).
[11] I. Baccarelli, A. Grandi, F. A. Gianturco, R. R. Lucchese, and N. Sanna, J. Phys. Chem. B **110**, 26240 (2006).
[12] T. C. Freitas, M. A. P. Lima, S. Canuto, and M. H. F. Bettega, Phys. Rev. A **80**, 062710 (2009).
[13] I. I. Fabrikant, S. Caprasecca, G. A. Gallup, and J. D. Gorfinkel, J. Chem. Phys. **136**, 184301 (2012).
[14] F. A. Gianturco and R. R. Lucchese, New J. Phys. **6**, 66 (2004).
[15] F. A. Gianturco and R. R. Lucchese, Eur. Phys. J. D **39**, 399 (2006).
[16] T. N. Rescigno, C. S. Trevisan, and A. E. Orel, Phys. Rev. Lett. **96**, 213201 (2006).
[17] C. S. Trevisan, A. E. Orel, and T. N. Rescigno, Phys. Rev. A **74**, 042716 (2006).
[18] V. Vizcaino, M. Jelisavcic, J. P. Sullivan, and S. J. Buckman, New J. Phys. **8**, 85 (2006).
[19] M. Allan, J. Phys. B **39**, 2939 (2006).
[20] M. H. F. Bettega, Phys. Rev. A **74**, 054701 (2006).
[21] M. Allan, Phys. Rev. Lett. **98**, 123201 (2007).
[22] T. N. Rescigno, C. S. Trevisan, and A. E. Orel, Phys. Rev. A **80**, 046701 (2009).
[23] G. A. Gallup, P. D. Burrow, and I. I. Fabrikant, Phys. Rev. A **80**, 046702 (2009).
[24] A. M. Scheer, P. Mozejko, G. A. Gallup, and P. D. Burrow, J. Chem. Phys. **126**, 174301 (2007).
[25] K. Coutinho and S. Canuto, J. Chem. Phys. **113**, 9132 (2000).

[26]B. M. Bode and M. S. Gordon, J. Mol. Graphics Modell. **16**, 133 (1998).
[27]K. Coutinho and S. Canuto, DICE, a Monte Carlo program for molecular liquid simulation, version 2.9, University of São Paulo, São Paulo, 2009.
[28]H. J. C. Berendsen, J. R. Grigera, and T. P. Straatsma, J. Phys. Chem. **91**, 6269 (1987).
[29]C. Møller and M. S. Plesset, Phys. Rev. **46**, 618 (1934).
[30]M. L. Leininger, W. D. Allen, H. F. Schaefer, and C. D. Sherrill, J. Chem. Phys. **112**, 9213 (2000).
[31]T. H. Dunning, Jr., J. Chem. Phys. **90**, 1007 (1989).
[32]M. J. Frisch, G. W. Trucks, H. B. Schlegel *et al*., GAUSSIAN 03, Revision D.01, Gaussian, Inc., Wallingford, CT, 2003.
[33]J. M. Briggs, T. B. Nguyen, and W. L. Jorgensen, J. Phys. Chem. **95**, 3315 (1991).
[34]C. M. Breneman and K. B. Wiberg, J. Comput. Chem. **11**, 361 (1990).
[35]G. Scalmani, M. J. Frisch, B. Mennucci, J. Tomasi, R. Cammi, and V. Barone, J. Chem. Phys. **124**, 094107 (2006).
[36]V. Manzoni, M. L. Lyra, R. M. Gester, K. Coutinho, and S. Canuto, Phys. Chem. Chem. Phys. **12**, 14023 (2010).
[37]M. V. A. Damasceno, B. J. C. Cabral, and K. Coutinho, Theor. Chem. Acc. **131**, 1214 (2012).
[38]K. Takatsuka and V. McKoy, Phys. Rev. A **24**, 2473 (1981); **30**, 1734 (1984).
[39]M. A. P. Lima, L. M. Brescansin, A. J. R. da Silva, C. Winstead, and V. McKoy, Phys. Rev. A **41**, 327 (1990).
[40]M. H. F. Bettega, L. G. Ferreira, and M. A. P. Lima, Phys. Rev. A **47**, 1111 (1993).
[41]G. B. Bachelet, D. R. Hamann, and M. Schlüter, Phys. Rev. B **26**, 4199 (1982).
[42]M. H. F. Bettega, A. P. P. Natalense, M. A. P. Lima, and L. G. Ferreira, Int. J. Quantum Chem. **60**, 821 (1996).
[43]T. H. Dunning, Jr., J. Chem. Phys. **53**, 2823 (1970).
[44]C. Bauschlicher, J. Chem. Phys. **72**, 880 (1980).
[45]R. F. da Costa, F. J. da Paixão, and M. A. P. Lima, J. Phys. B **37**, L129 (2004); **38**, 4363 (2005).
[46]C. G. Gray and K. E. Gubbins, *Theory of Molecular Fluids. Volume 1: Fundamentals* (Clarendon Press, Oxford, 1984).
[47]M. W. Schmidt, K. K. Baldridge, J. A. Boatz, S. T. Elbert, M. S. Gordon, J. H. Jensen, S. Koseki, N. Matsunaga, K. A. Nguyen, S. J. Su, T. L. Windus, M. Dupuis, and J. A. Montgomery, J. Comput. Chem. **14**, 1347 (1993).
[48]S. W. Staley and J. T. Strnad, J. Phys. Chem. **98**, 116 (1994).
[49]T. C. Freitas, M. T. do N. Varella, R. F. da Costa, M. A. P. Lima, and M. H. F. Bettega, Phys. Rev. A **79**, 022706 (2009).
[50]R. Rivelino, B. J. C. Cabral, K. Coutinho, and S. Canuto, Chem. Phys. Lett. **407**, 13 (2005).
[51]S. Miertuš, E. Scrocco, and J. Tomasi, Chem. Phys. **55**, 117 (1981).
[52]E. Cancès, B. Mennucci, and J. Tomasi, J. Chem. Phys. **107**, 3032 (1997).
[53]W. J. Hehre, L. Radom, P. v. R. Schleyer, and J. A. Pope, *Ab Initio Molecular Orbital Theory*, 1st ed. (John Wiley and Sons, New York, 1986).
[54]F. Jensen, *Introduction to Computational Chemistry*, 2nd ed. (John Wiley and Sons, West Sussex, 2007).